Regional production prediction technology based on gravity and magnetic data from the Eagle Ford formation, Texas, USA

Ivan Priezzhev, Aaron Scollard, and Zhengang Lu, Schlumberger*

Summary

An unconventional production data analysis technology that uses on gravity and magnetic data was applied to the Eagle Ford formation. The prediction technology uses a neural network with multivariate input and multivariate output and is based on an evolutionary algorithm for neural network teaching. Simultaneously, multivariate neural network output allows for predicting several parameters, such as oil, gas, and water production rates. This prediction is based on multivariate Gaussian distribution theory and an objective function, in this case, Mahalanobis distance versus square distance for one-parameter prediction. In addition, we applied gravity and magnetic depth decomposition technology based on potential field inverse theory.

Introduction

Regional sweet spot analysis on the basis of production data analysis versus geological maps and other data sets, especially for unconventional resources has always been of great interest (Roth et al., 2012). In developing an analysis technology for production prediction, our intent was to use only an independent dataset for the prediction. A porosity map created from well log porosity values in the target interval, for example, is not completely independent from production because production data are dependent on the average porosity for the wells in the target interval. The porosity map will have very high correlation with the production data, but it will not be useful for predicting new areas for production because there is no additional information between wells. Other similar parameters created from well logs also will be originally depended to production rates. On the other hand, a seismic dataset is absolutely independent from production; seismic attributes have good correlation with production rates and so can be effectively used for production prediction.

For many cases, especially for regional investigations, we do not have seismic dataset that covers all of the area of interest. In these cases, we can use gravity and magnetic data as an independent observation. To use the data more effectively, we propose to apply a simple inversion technique that allows us to calculate the 3D distribution of the density contrast parameters, which can have a better correlation to the production data from the target layer.
We also applied a simultaneous-prediction technique for several parameters such as oil, gas, and water production. Simultaneous prediction for multivariate output requires minimization of the square difference together with crosscorrelation between predictive output parameters. This allows for prediction without the influence of the strong correlation between predicted parameters.

Method

For this prediction method, we used technology based on a nonlinear neural network (Figure 1) that can be built using a multivariate Gaussian distribution theory and which allows for simultaneous prediction of several parameters (for example: oil, gas, and water rates).

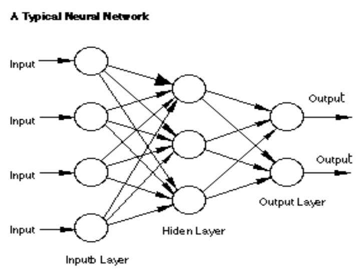

Figure 1: Multi-input and multi-output neural network with one hidden layer.

For multi-outputs, it is not enough to minimize just the square difference because with a multivariate Gaussian distribution, the objective function must include the crosscorrelation between output datasets. Let $X_i^k,\ i = 1,\dots,N,\ k = 1,\dots,K$ define measured values of the predictive parameters, where N is the number of wells used for learning, K is number of predicted parameters, and $\overline{X_i^k}$ correspond to predicted values. The objective function for neural network learning will be the following:

$$M\left(X_i^k - \overline{X_i^k}\right) = \left(X_i^k - \overline{X_i^k}\right)^T \mathbf{S}^{-1} \left(X_i^k - \overline{X_i^k}\right), \qquad (1)$$

where **S** is a crosscorrelation matrix between measured and predicted parameters (for example oil, gas, and water rates). Function $M\left(X_i^k - \overline{X_i^k}\right)$ is usually called the Mahalanobis distance (Mahalanobis, 1927).

In many cases, gravity or magnetic maps do not show a good correlation with production data because the maps usually show the sum of the effects from different depths. We propose to use a simple inversion technique that allows

DOI http://dx.doi.org/10.1190/segam2014-0289.1

us to decompose these data to different depth sources. Only gravity and magnetic sources close to the target layer will be used for prediction. The gravity and magnetic depth decomposition technology that we used for prediction is based on the Kobrunov and Varfolomeev (1981) equation for density distribution in the wavenumber domain:

$$D(\omega_1,\omega_2,z) = \frac{1}{\gamma} G(\omega_1,\omega_2,0) \frac{K(\omega_1,\omega_2,z)}{\int_{z'=0}^{\infty} K(\omega_1,\omega_2,z') e^{-rz'} dz'}, \quad (2)$$

where $D(\omega_1,\omega_2,z)$ is density spectrum on depth = z,
$G(\omega_1,\omega_2,0)$ is spectrum of the observed gravity field,
$K(\omega_1,\omega_2,z)$ is the function that describes the density spectrum relation versus depth (z),
ω_1,ω_2 are wavenumbers corresponding to x, y,
$r = \sqrt{\omega_1{}^2 + \omega_2{}^2}$ is the radial wavenumber,
γ is the gravity constant.

Another form of this equation is $D(\omega_1,\omega_2,z) = G(\omega_1,\omega_2,0)H(\omega_1,\omega_2,z)$, where, $H(\omega_1,\omega_2,z)$ is the inversion operator in the wavenumber domain.
Equation 2 is fundamental for understanding the nature of the gravity, or any other potential field, inversion and non-uniqueness. We can use any function $K(\omega_1,\omega_2,z)$ to get the corresponding density contrast distribution $D(\omega_1,\omega_2,z)$ if the spectrum can be transferred back to the spatial domain. For example, if all sources of the gravity field are distributed within the depth interval from z_1 to z_2, which means, $K(\omega_1,\omega_2,z) = 1, if\ z_1 \le z \le z_2$, then $H(\omega_1,\omega_2,z) = \frac{r}{\gamma(e^{-rz_1}+e^{-rz_2})}$. There also exist many other similar examples to get simple equations (Kobrunov and Varfolomeev, 1981).

We propose to use $K(\omega_1,\omega_2,z) = \omega^n e^{-n\omega z}$, which is the vertical *n*-derivation of the gravity field from a singular source; the inversion operator is then (Priezzhev, 1989, 2005)

$$H(\omega_1,\omega_2,z,n) = \frac{1}{\gamma}\frac{(n+1)^{n+1}}{!n} z^n r^{n+1} e^{-nrz}. \quad (3)$$

The inversion operator, equation 3, has a maximum $r = \frac{1}{z}$ and looks like a band frequency filter for the sources on depth. Parameter *n* can be used for the slope of the filter curve (Figure 2).

On the other hand, equation 3 is an inversion operator because it corresponds to equation 2, which means the density distribution calculated by means of equation 3 will exactly correspond to the observed field if we use forward modeling.

Figure 2 demonstrates the spectra of inversion operators in accordance with equation 3 for different depths, showing the band-filtering nature of spectra. Figure 3 shows a synthetic example for using equation 3 to calculate the depth density distribution of the gravity field. The synthetic example shows the ability and limitations of the method to detect and separate sources of the gravity field.

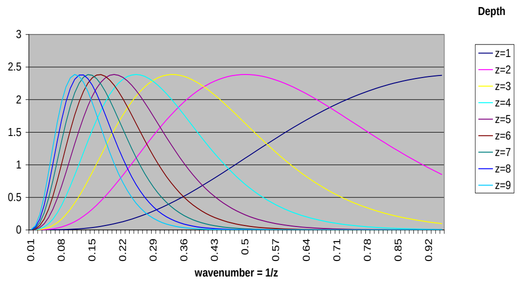

Figure 2: Spectra of inversion operator, equation 3, for different depths.

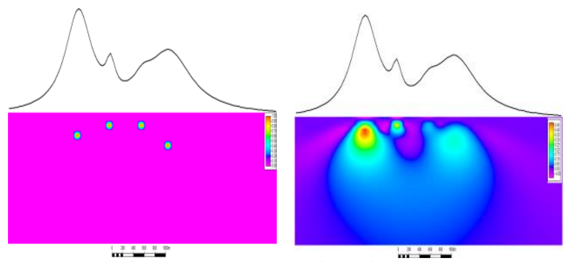

Figure 3: Left, synthetic gravity field from four sources (size 10x10 m, depth from left to right, 200 m, 100 m, 150 m, 300 m, with corresponding density contrast of 1, 0.7, 0.5, and 1 g/cm^3, respectively). Right, density contrast distribution according equation 3 Maximum gravity field is 0.008 mGal.

We can apply the same equations and the same approach for the inversion of magnetic data to calculate magnetic source parameters (relative magnetization or magnetic "density" contrast). The difference lies only in the following:

- We transfer magnetic data to the pole according Baranov's algorithm (Baranov, 1957). To do this, we must know the vector of the Earth's normal magnetization (usually in form of dip and azimuth).
- We must calculate pseudo gravity from magnetic data. This means that we need to fulfil an integration operation or be in a wavenumber domain, thus, we must use the following additional multiplier $\frac{1}{ir}$, where $i = \sqrt{-1}$.

For production prediction in the Eagle Ford formation, we use density contrasts calculated from equation 3 around the target layer within a defined radius of 500 feet based on both gravity and magnetic fields. To teach the neural network, we use an evolutionary algorithm with the objective function, equation 1 for simultaneous prediction of several parameters: average oil, gas, and water rates for 1 year. Application of the evolutionary algorithm allows us to find a solution that can be very close to a global minimum of the objective function.

The number of neurons in the hidden layer of the neural network gives the advantage of managing the power of the nonlinearity. If the number of neurons is zero, the network creates a simple linear prediction operator (linear regression).

DOI http://dx.doi.org/10.1190/segam2014-0289.1

To eliminate the "overlearning" effect that causes instability and nonuniqueness for the prediction operator, we use the Tikhonov regularization method (Tikhonov and Arsenin, 1977) to stabilize the prediction operator. For this purpose, we add Tikhonov stabilization to the objective function, equation 1:

$$M\left(X_i^k - \overline{X_i^k}\right) + \alpha \sum_{i=1}^{N} c_i{}^2 \qquad (4)$$

where c_i is neural network coefficient

N is number of all neural network coefficients and thresholds,

$\alpha > 0$ is the regularization parameter of Tikhonov, which can be defined empirically

Minimization of equation 4 does not allow the neural network to create very high contrast coefficients, and that creates more stable prediction results.

Eagle Ford Example

For the production data analysis, we used about 45,000 production wells from the Eagle Ford formation, Texas, USA, with 1- year average production rates for oil, gas, and water. All production data were downloaded from an IHS database. In Figure 3, the satellite gravity field (Sandwell and Smith, 2009; Sandwell *et al*., 2013) is shown, and in Figure 4, the magnetic field (Maus *et al*., 2009) is presented. Figures 5 and 6 demonstrate the 3D distribution of density contrast and magnetic "density" contrast calculated via equation 3. From a visual analysis of the gravity and magnetic maps, it can be clearly seen that the production wells are commonly positioned on the gradient of these fields. In 3D view, this position corresponds to negative density contrast for gravity inversion results and negative magnetic "density" contrast for magnetic field inversion results.

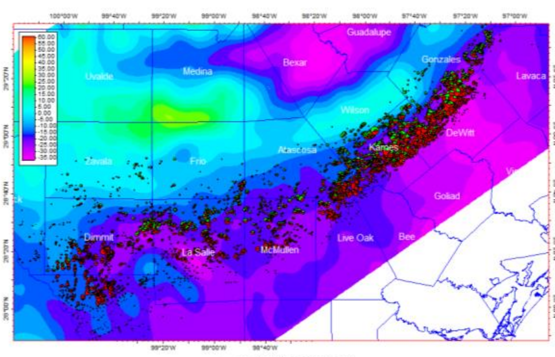

Figure 3: Satellite gravity field (mGal) and 45,000 production wells in the Eagle Ford. Green sectors in pie charts are cumulative oil production, red sectors are cumulative gas production, and size of pie charts is cumulative oil production.

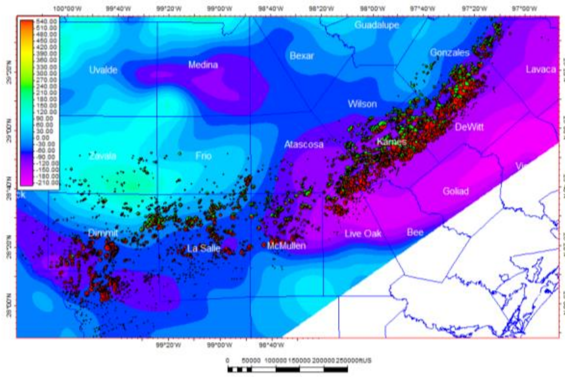

Figure 4: Magnetic field and 45,000 production wells in the Eagle Ford. Green sectors in pie charts are cumulative oil production, red sectors are cumulative gas production, and size of pie charts is cumulative oil production.

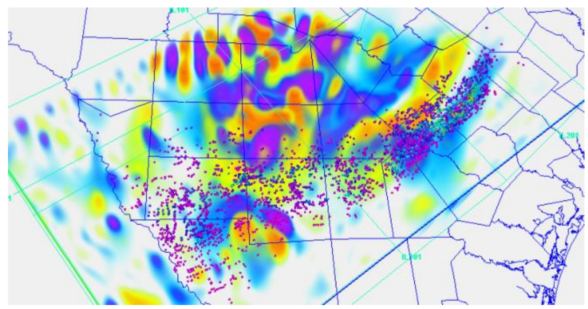

Figure 5: 3D view of the density contrast distribution (red is positive and blue is negative) according equation 3 and production wells (colored spheres) in the Eagle Ford.

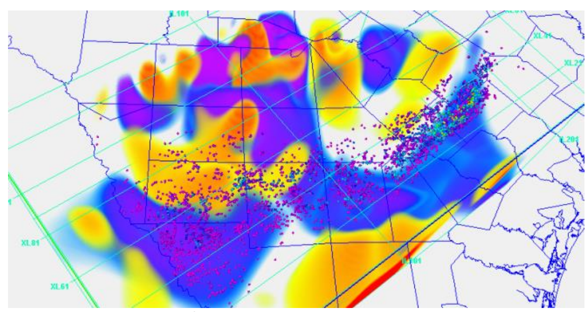

Figure 6: 3D view of the magnetic "density" contrast distribution (red is positive and blue is negative) according equation 3 and production wells (colored spheres) in the Eagle Ford.

Figures 7 and 8 demonstrate oil and gas production prediction results based on the neural network (three neurons in hidden layer) from the gravity and magnetic-density distribution around the Eagle Ford target layer. The final correlation coefficient was 0.63 for oil production prediction and 0.55 for gas production prediction for the entire Eagle Ford area studied. If use only central and eastern parts of Eagle Ford area then the correlation coefficient will be 0.89 and 0.75 correspondently for oil and gas production rates. For both parameters, oil and gas

DOI http://dx.doi.org/10.1190/segam2014-0289.1

production rates, we used the 1-year cumulative value for each well.

The cross section in Figure 9 shows the density contrast and gravity, magnetic, and production prediction results**.** The position of wells with good oil production in Figure 9 has a very clear correlation with negative density contrast.

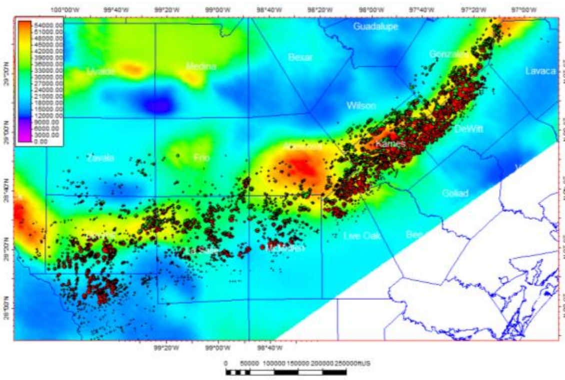

Figure 7: Oil production prediction map and production wells in the Eagle Ford. Size of pie charts is cumulative oil production.

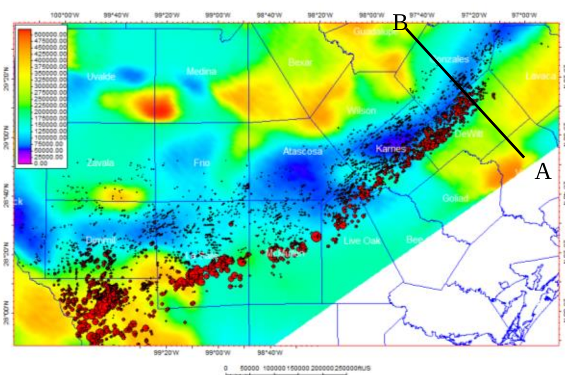

Figure 8: Gas production prediction map and production wells in the Eagle Ford. Size of pie charts is cumulative gas production.

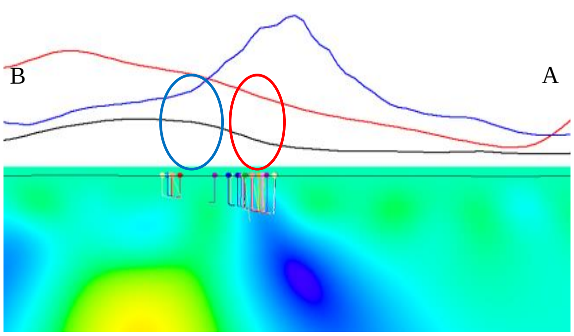

Figure 9: Cross section with density contrast distribution (red is positive and blue is negative) along line A-B (see position on Figure 8). The black curve is the gravity field, and the red curve is the magnetic field. The blue curve is the oil production prediction. The red ellipse shows good oil producer, and blue ellipse shows poor oil producers.

Conclusions

The proposed technology enables a user to simultaneously predict multiple parameters (such as oil, gas, and water production) for the target formation in an unconventional reservoir. To identify the sweet spot, a variety of independent inputs (seismic data, gravity data, magnetic attributes, etc.) can be applied. To achieve better correlation of the production data and gravity and magnetic fields, a simple inversion technology is proposed to calculate the volume of density contrast close to target layer. The primary advantages of using a nonlinear operator based on a neural network and evolutionary algorithm are as follows:

- The technique gives us the ability to simultaneously predict several variables (such as oil, gas, and water production rates).
- The iterative search for solutions is based on an evolutionary algorithm that finds a solution very close to a global minimum.
- Simultaneous prediction for multivariate output requires minimization of the square difference together with crosscorrelation between predictive output parameters (oil, gas, and water rates). This allows for prediction without the influence of the strong correlation.
- The degree of nonlinearity of the relationships can be managed through the dimension of the hidden layer. If there is no hidden layer, searching is done by linear regression. Linear and nonlinear regression and the neural network have the same nature and, also, the same problems of instability and nonuniqueness.
- The instability and nonuniqueness can be eliminated using a Tikhonov stabilization approach. The technique has the advantage of a lack of sensitivity to the huge number of highly correlated input attributes because neural networks can automatically compensate for the highly correlated input through thresholds for input coefficients and using the regularization technique.

Acknowledgments

The authors thank Schlumberger for the opportunity to develop this technique and for the permission to publish the results of the work. This work also includes production data supplied by IHS; Copyright (2014) IHS Energy Log Services Inc.

DOI http://dx.doi.org/10.1190/segam2014-0289.1

http://dx.doi.org/10.1190/segam2014-0289.1

EDITED REFERENCES

Note: This reference list is a copy-edited version of the reference list submitted by the author. Reference lists for the 2014 SEG Technical Program Expanded Abstracts have been copy edited so that references provided with the online metadata for each paper will achieve a high degree of linking to cited sources that appear on the Web.

REFERENCES

Kobrunov, A. I., and V. A. Varfolomeev, 1981, One approach of density equivalent representation and using it for gravity field interpretation: Earth Physics USSR Academy of Science (in Russian).

Mahalanobis, P. C., 1925, Analysis of race-mixture in Bengal: Journal and Proceedings of the Asiatic Society of Bengal, **23**, 301–333, http://hdl.handle.net/10263/1622.

Maus, S., U. Barckhausen, H. Berkenbosch, N. Bournas, J. Brozena, V. Childers, F. Dostaler, J. D. Fairhead, C. Finn, R. R. B. von Frese, C. Gaina, S. Golynsky, R. Kucks, H. Lühr, P. Milligan, S. Mogren, R. D. Müller, O. Olesen, M. Pilkington, R. Saltus, B. Schreckenberger, E. Thébault, and F. Caratori Tontini, 2009, EMAG2: A 2-arc min resolution earth magnetic anomaly grid compiled from satellite, airborne, and marine magnetic measurements: Geochemistry, Geophysics, Geosystems, **10**, no. 8, Q08005, http://dx.doi.org/10.1029/2009GC002471.

Priezzhev, I., 1989, Spectral and statistical analyses of aero geophysical data in system ASOM-AGS/ES: Ph.D. dissertation, Moscow State Geological Prospecting Academy (in Russian).

Roth, M., R. Peebles, and T. Royer, 2012, Sweetspot mapping in the Eagle Ford with multi-volume seismic analysis: Presented at the 18th Annual 3D Seismic Symposium, https://www.transformsw.com/wp-content/uploads/2013/05/Sweetspot-Mapping-in-the-Eagle-Ford-with-Multi-Volume-Seismic-Analysis-2012-RMAG-3D-Symposium-Peebles-Royer-and-Roth.pdf.

Sandwell, D. T., E. Garcia, K. Soofi, P. Wessel, M. Chandler, and W. H. F. Smith, 2013, Toward 1-mGal accuracy in global marine gravity from CryoSat-2, Envisat, and Jason-1: The Leading Edge, **32**, 892–899, http://dx.doi.org/10.1190/tle32080892.1.

Sandwell, D. T., and W. H. F. Smith, 2009, Global marine gravity from retracked Geosat and ERS-1 altimetry: Ridge segmentation versus spreading rate: Journal of Geophysical Research: Solid Earth, **114**, no. B1, B01411, http://dx.doi.org/10.1029/2008JB006008.

Tikhonov, A. N., and V. Y. Arsenin, 1977, Solution of ill-posed problems: Winston & Sons.